Protein kinase C epsilon is required for macrophage activation and defense against bacterial infection

Castrillo, A; Pennington, DJ; Otto, F; Parker, PJ; Owen, MJ; Bosca, L

Protein Kinase Cε Is Required for Macrophage Activation and Defense Against Bacterial Infection

Antonio Castrillo,[1] Daniel J. Pennington,[2] Florian Otto,[3] Peter J. Parker,[2] Michael J. Owen,[2] and Lisardo Boscá[1]

[1]*Instituto de Bioquímica (Centro Mixto Consejo Superior de Investigaciones Cientificas-UCM), Facultad de Farmacia, Universidad Complutense, 28040 Madrid, Spain*
[2]*Imperial Cancer Research Fund, London WC2A 3PX, United Kingdom*
[3]*Universitaetsklinik, Nothnagel-Laboratorien, D-79106 Freiburg, Germany*

Abstract

To assess directly the role of protein kinase C (PKC)ε in the immune system, we generated mice that carried a homozygous disruption of the PKCε locus. PKCε$^{-/-}$ animals appeared normal and were generally healthy, although female mice frequently developed a bacterial infection of the uterus. Macrophages from PKCε$^{-/-}$ animals demonstrated a severely attenuated response to lipopolysaccharide (LPS) and interferon (IFN)γ, characterized by a dramatic reduction in the generation of NO, tumor necrosis factor (TNF)-α, and interleukin (IL)-1β. Further analysis revealed that LPS-stimulated macrophages from PKCε$^{-/-}$ mice were deficient in the induction of nitric oxide synthase (NOS)-2, demonstrating a decrease in the activation of IκB kinase, a reduction in IκB degradation, and a decrease in nuclear factor (NF)κB nuclear translocation. After intravenous administration of Gram-negative or Gram-positive bacteria, PKCε$^{-/-}$ mice demonstrated a significantly decreased period of survival. This study provides direct evidence that PKCε is critically involved at an early stage of LPS-mediated signaling in activated macrophages. Furthermore, we demonstrate that in the absence of PKCε, host defense against bacterial infection is severely compromised, resulting in an increased incidence of mortality.

Key words: nitric oxide • protein kinase C • nitric oxide synthase • macrophage activation • bacterial infection

Introduction

The protein kinase C (PKC)* family of serine/threonine kinases consists of at least 11 closely related isoenzymes that can be subdivided into three groups (1). The classical isotypes are calcium and diacylglycerol dependent, and include PKCα, PKCβI and βII, and PKCγ. The novel isotypes are also diacylglycerol dependent, but are calcium independent. These include PKCδ, PKCε, PKCθ, and PKCη (2). The atypical isotypes, comprising of PKCζ and PKCλ/ι, are nonresponsive to diacylglycerol. In any one tissue several isoenzymes can be expressed, and redundancy of function has often hampered the identification of definitive roles for individual family members. Nevertheless, in recent years, mice deficient for PKCβ (both βI and βII), PKCγ, PKCθ, and PKCε have all been generated, and the analysis of these animals has increasingly highlighted the essential nonredundant roles for PKC isoenzymes in many systems (3–6).

Several of the reported phenotypes for PKC mutant mice have identified a role for a specific isoenzyme in the cells of the immune system. For example, mice deficient for PKC βI and βII have a marked immunodeficiency that is characterized by an attenuated humoral immune response specifically associated with an impairment of signaling through the B cell receptor (4). In contrast, mice deficient for PKCθ have a defect in T cell receptor signaling, which results in a severe decrease in nuclear factor (NF)κB activation and mature T cell proliferation (6).

A number of in vitro and ex vivo studies have also implicated a role for PKCε in the regulation of the immune system. In immature thymocytes, it was suggested that PKCε

A. Castrillo and D.J. Pennington contributed equally to this work.

Address correspondence to Lisardo Boscá, Instituto de Bioquímica, Facultad de Farmacia, 28040 Madrid, Spain. Phone: 34-91394-1853; Fax: 34-91544-7254; E-mail: boscal@eucmax.sim.ucm.es

**Abbreviations used in this paper:* ERK, extracellular signal–regulated kinase; IKK, IκB kinase; MAP, mitogen-activated protein; NAK, NFκB-activating kinase; NF, nuclear factor; NOS, nitric oxide synthase; PKC, protein kinase C; TLR, Toll-like receptor.

was involved in glucocorticoid-induced apoptosis (7), while in mature T cell lines, PKCε activation was implicated in signaling through the high-affinity IL-2 receptor (8). Much evidence also exists to suggest that PKCε could be an important mediator of macrophage function. For example, it was demonstrated using several complementary experimental approaches that the macrophage-specific inhibition of PKCε was partly responsible for the antiinflammatory action of IL-4 (9). In addition, the expression of PKCε was shown to be sufficient for NO production in the RAW 264.7 macrophage cell line (10), while a number of studies have suggested that the activation of PKCε is a critical event in the signaling response of primary macrophages to either LPS (11, 12), or GM-CSF (13). Furthermore, it was recently demonstrated that PKCε is required for the induction of mitogen-activated protein kinase phosphatase-1 in LPS-stimulated macrophages (14), and that macrophage phagocytosis is dependent on the activation of a nPKC, specifically PKCε (15).

To address directly whether PKCε has a role in the function of the various cell types of the immune system, we generated and characterized mice with a targeted disruption of the PKCε gene. Thymocyte apoptosis, T cell proliferation, and B cell function were all comparable to that observed in control littermates. However, even though circulating monocytes were present at wild-type levels, and maturation and homing of these cells appeared normal, elicited peritoneal macrophages generated significantly lower levels of NO, TNFα, and IL-1β in response to LPS and IFNγ stimulation. We demonstrate that LPS-treated macrophages from PKCε$^{-/-}$ mice failed to induce nitric oxide synthase-2 (NOS-2) expression and showed a significant reduction in the activation of both IκB kinase (IKK) and NFκB. The p44 and p42 extracellular signal–regulated kinase (ERK) kinases and the p38 mitogen-activated protein (MAP) kinases were also activated to a considerably lesser extent in PKCε$^{-/-}$ cells. In addition, we demonstrate that PKCε$^{-/-}$ mice displayed a significant increase in sensitivity and mortality in response to either an intravenous Gram-negative or Gram-positive bacterial infection. Taken together, these data implicate PKCε as a critical component of the LPS signaling cascade in activated macrophages, and highlights the importance of this gene in mounting an effective immune response to various bacterial pathogens.

Materials and Methods

Chemicals. Reagents were from Sigma-Aldrich, Roche, and Merck. For cytokine assays Biotrak kits were from Amersham Pharmacia Biotech. Cytokines were from Roche. LPS was from *Salmonella typhimurium* (Sigma-Aldrich). Serum and other cell culture reagents were from BioWhittaker. Antibodies were from Santa Cruz Biotechnology, Inc. and from New England Biolabs, Inc.

Generation of PKCε$^{-/-}$ Mice. A 9.3-kb EcoRI fragment containing the first exon of the PKCε gene was isolated from a murine 129/Sv genomic DNA library (gift from T. Rabbitts, Laboratory of Molecular Biology, Cambridge). A targeting vector was generated by introducing a positive selectable cassette into the PstI site of exon 1. This cassette contains stop codons in all three frames, an independent ribosomal entry site (IRES) followed by the *LacZ* gene with an SV40 polyadenylation sequence, and a neomycin phosphotransferase gene (MC1Neo poly(A); gift from A. Smith, Centre for Genome Research, Edinburgh, UK). Correctly targeted GK129 ES cells (see Fig. 1 for Southern blot details) were injected into C57BL/6 blastocysts. Chimeric mice were bred to C57BL/6 mice in specific pathogen-free (SPF) conditions to generate PKCε homozygous mutant animals. PKCε$^{-/-}$ and PKCε$^{+/-}$ mice were maintained on a mixed C57Bl/6 × 129/Sv genetic background and were genotyped by Southern blot (Fig. 1, A and B) or PCR analysis of tail DNA (data not shown). Mice were fed ad libitum with a standard diet (Panlab) and kept under a light and dark cycle of 12 h (lights on at 8 a.m.).

Preparation of Peritoneal Macrophages. 4 d before use, mice were injected intraperitoneally with 1 ml of sterile 3% (wt/vol) thioglycollate (16). After sacrificing the animals, the peritoneal cavity was flushed with 10 ml of sterile RPMI 1640. The peritoneal cell suspension was carefully aspirated avoiding hemorrhage and kept at 4°C to prevent the adhesion of the macrophages to plastic. Cells were recovered by centrifugation at 200 *g* for 10 min and washed twice with 25 ml of ice-cold PBS. Cells were seeded at 10^6/cm^2 in RPMI 1640 supplemented with 10% heat-inactivated FCS and 50 μg/ml of gentamicin, penicillin, and streptomycin. After incubation for 1 h at 37°C in a 5% CO_2 atmosphere, nonadherent cells were removed by extensive washing with PBS. Experiments were performed in phenol red-free RPMI 1640 supplemented with 0.5 mM arginine and 10% heat-inactivated FCS plus antibiotics and agonists as indicated in the figures and legends (16). For in vivo experiments, animals were injected intraperitoneally with 0.5 ml of a solution containing LPS from *S. typhimurium* and D-galactosamine (17, 18). An *Escherichia coli* (strain ATCC 25922) or *Staphylococcus aureus* (strain ATCC 6538P) suspension in PBS was quantified and administered (0.5 ml) through the tail vein.

Flow Cytometric Analysis. Cells were stained with PE-labeled antimurine CD11b (clone M1/70) and FITC-labeled anti-CD14 (clone rmC5–3) from BD PharMingen and analyzed on a FACScan™ cytometer (Becton Dickinson) equipped with a 25-mW argon laser. Analysis of apoptotic cells was performed by propidium iodide staining, following a previous protocol (19, 20). The quantification of the percentage of apoptotic cells was done using a dot plot of the forward scatter against the phosphatidylinositol fluorescence. Cell sorting and analysis of viable and apoptotic populations was performed to confirm the criteria of gating (20).

Preparation of Blood Samples for Cytokine and PGE_2 Assay. Blood was collected from the tail vein or by cardiac puncture at the indicated times and the levels of TNFα, IL-1β, and PGE_2 were assayed using an enzyme immunoassay kit, following the suppliers recommendations (Biotrak; Amersham Pharmacia Biotech).

Determination of NO Synthesis. NO release was determined spectrophotometrically by the accumulation of nitrite and nitrate in the medium (phenol red-free). Nitrate was reduced to nitrite as described (16). Nitrite levels were determined with Griess reagent. Results are expressed as the amount of nitrite and nitrate released per mg of cell protein.

Preparation of Cell Extracts. Adhered macrophages were washed twice with ice-cold PBS and the plates (6-cm diameter) were filled with 0.4 ml of buffer A (20 mM Tris-HCl, pH 7.8; 5 mM $MgCl_2$, 10 mM KCl, 0.5 mM EGTA, 1 mM phenylmethylsulfonyl fluoride, 0.5 mM dithiothreitol, and 10 μM leupeptin). The cells were scraped off the dishes using a rubber policeman

and mixed with one volume of a 1% Nonidet P-40 solution. The tubes were gently vortexed for 15 s and nuclei were sedimented by centrifugation at 8,000 *g* for 15 s. Aliquots of the supernatant were stored at −80°C (cytosolic extracts), and the nuclear pellets were resuspended in 100 μl of buffer A supplemented with 0.4 M KCl. Nuclear proteins were extracted by centrifugation at 13,000 *g* for 15 min and aliquots of the supernatant were stored at −80°C (16). Proteins were measured using the Bio-Rad Laboratories detergent-compatible protein reagent. All steps of cell fractionation were performed at 4°C.

Measurement of IKK2 Activity. Cells (10^7) were homogenized in buffer A and centrifuged at maximal speed for 10 min in a microcentrifuge. The supernatant (1 ml) was precleared and IKK2 was immunoprecipitated with 1 μg of anti-IKK2 Ab (21). After five washes of the immunoprecipitate with buffer A, the pellet was resuspended in kinase buffer (20 mM HEPES, pH 7.4; 0.1 mM EDTA, 100 mM NaCl, 1 mM DTT, 0.5 mM PMSF, 2 μg/ml aprotinin, 10 μg/ml leupeptin, 2 μg/ml TLCK, 5 mM NaF, 1 mM $NaVO_4$, 10 mM Na_2MoO_4 and 10 nM okadaic acid). Kinase activity was assayed in 100 μl of buffer A containing 100 ng of immunoprecipitation, 50 μM [γ-^{32}P]ATP (0.5 μCi), and using as substrate 100 ng of GST-IκBα (amino acids 1–54). Controls with the corresponding S32A and S36A mutated protein were unable to be phosphorylated under these conditions (data not shown). Aliquots of the reaction were stopped at various time points with 1 ml of ice-cold buffer A supplemented with 5 mM EDTA. The linearity of the kinase reaction was confirmed over a period of 30 min.

Electrophoretic Mobility Shift Assays. An oligonucleotide corresponding to the proximal κB motif of the murine NOS-2 promoter (22, 23) 5′-CCAACTGGGGACTCTCCCTTTGGGAACA-3′, and one corresponding to the PPARα binding site of the promoter of acyl-CoA oxidase (24) 5′-CGAACGTGACCTTTGTCCTCCCCTTTTGCTCGATC-3′, were annealed with complementary sequence (50 ng) and labeled with Klenow enzyme in the presence of 50 μCi of [α-^{32}P]dCTP plus unlabeled dNTPs to a final volume of 50 μl. The probes were precipitated with ethanol and extracted with phenol/chloroform. DNA binding assays of nuclear extracts were performed by incubating for 30 min at 4°C, 5×10^4 dpm of the DNA probe with 5 μg of nuclear protein, 1 μg/ml of poly(dI·dC), 5% glycerol, 1 mM EDTA, 100 mM KCl, 5 mM $MgCl_2$, 1 mM dithiothreitol, and 10 mM Tris-HCl, pH 7.8, in a final volume of 20 μl. The incubation mixture was applied to a 6% polyacrylamide gel that had been electrophoresed previously for 30 min at 100 V. Gels were electrophoresed at 0.8 volts/cm^2 in 45 mM Tris-borate, followed by vacuum-transference to 3MM Whatman paper and quantification of the band intensities in an autoradiograph (Fuji Bas 1000). Analysis of competition with unlabeled oligonucleotides was performed using a 20-fold excess of double stranded DNA in the binding reaction, and adding the nuclear extracts as the last step in the binding assay. Supershift assays were performed after addition of antibodies (0.5 μg) to the binding reaction and incubation for 1 h at 4°C (22).

Western Blot Analysis. Cytosolic and nuclear extracts were obtained as described previously (22). Samples containing equal amounts of protein (30 μg and 10 μg per lane of cytosolic and nuclear extracts, respectively) were boiled in 250 mM Tris-HCl, pH 6.8, 2% SDS, 10% glycerol, 2% β-mercaptoethanol, and size-separated in 10% SDS-PAGE. The gels were processed as recommended by the supplier of the antibodies against various murine antigens (NOS-2, IκBα, phospho(S^{32})IκBα, p38 and p42/p44 MAP kinases, p50, and p65; from Santa Cruz Laboratories or New England Biolabs, Inc.) and after blotting onto a polyvinylidine difluoride (PVDF) membrane, proteins were revealed following the enhanced chemoluminescence (ECL) technique (Amersham Pharmacia Biotech). Different exposure times of the films were used to ensure that bands were not saturated. Quantification of the films was performed by laser densitometry (Molecular Dynamics). Westerns for PKC were as described previously (see reference 10).

RNA Extraction and Analysis. Total RNA ($2–4 \times 10^6$ cells) was extracted following the guanidinium thiocyanate method (Trizol; GIBCO BRL). For Northern blot analysis equal amounts of RNA were denatured and size-separated by electrophoresis in a 0.9% agarose gel containing 2% formaldehyde and MOPS buffering system as described previously (22). The RNA was transferred to Nytran membranes (NY 13-N; Schleicher & Schuell) with 10× SSC (1.5 mM NaCl, 0.3 mM sodium citrate, pH 7.4). An 817-bp fragment (nucleotides 1 to 817) from the cDNA of murine NOS-2 was labeled as a probe with the Rediprime kit (Amersham Pharmacia Biotech). The intensity of the bands was quantified in a Fuji BAS1000 autoradiograph using hybridization with a ribosomal 18S probe as an internal control. For reverse transcription (RT)-PCR, cDNA was generated from 10 μg of total RNA using the SMART cDNA synthesis technique (CLONTECH Laboratories, Inc.). A standard 30 cycle PCR was then performed on one hundredth of the starting sample using the following primers; PKCε(F) 5′-GCCAAAGTGCTGGCTGACCTTGG-3′, PKCε(R) 5′-CGGCATAGAACCGAGAACGAGGC-3′, β-act(F) 5′-TGCCTGACGGCCAGGTCATCA-3′, β-act(R) 5′-CGGACTCGTCATACTCCTGC-3′. An annealing temperature of 62°C was used for both PCRs (Advantage 2; CLONTECH Laboratories, Inc.).

Statistical Analysis. The data shown are the means ± SEM of the number of experiments or animals indicated. The product limit of the cumulative survival (Kaplan-Meier) was calculated with the Log-rank test for all survival data using the SPSS 10.0 software. Statistical significance was estimated with analysis of variance (ANOVA) and Student's *t* test for unpaired observations, using commercially available software (SPSS). A *P* value of less than 0.05 was considered significant.

Results

Generation of Mice Deficient for PKCε. Several recent studies have strongly implicated PKC, and more specifically PKCε, in various aspects of the maturation and function of the immune system. To address these issues directly, mice deficient for PKCε were generated by inserting a LacZ/Neo sequence into the first exon of the PKCε gene (Fig. 1 A). ES cells (data not shown) and mice heterozygous or homozygous for the PKCε mutation were assessed by Southern blot analysis for a correct targeting event (Fig. 1, A and B). RT-PCR (Fig. 1 C), Northern blot analysis (data not shown), and Western blot analysis confirmed that PKCε mRNA and protein were absent at this level of detection, whereas protein levels for other PKC isoenzymes remained unaltered (Fig. 1 D).

After heterozygous mating, PKCε$^{-/-}$ mice were born at the expected Mendelian frequency, with life expectancy no different to wild-type littermates. PKCε-deficient animals were, however, 10–15% smaller than controls,

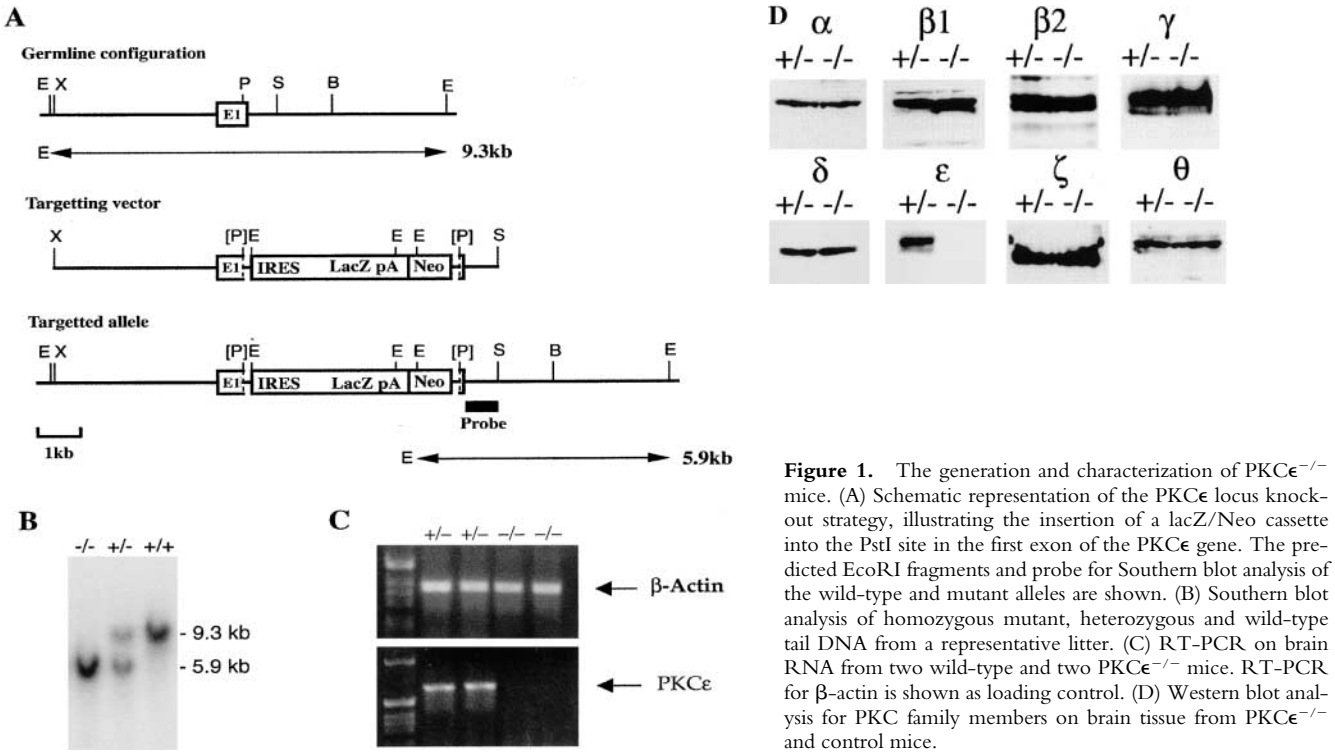

Figure 1. The generation and characterization of PKCε$^{-/-}$ mice. (A) Schematic representation of the PKCε locus knockout strategy, illustrating the insertion of a lacZ/Neo cassette into the PstI site in the first exon of the PKCε gene. The predicted EcoRI fragments and probe for Southern blot analysis of the wild-type and mutant alleles are shown. (B) Southern blot analysis of homozygous mutant, heterozygous and wild-type tail DNA from a representative litter. (C) RT-PCR on brain RNA from two wild-type and two PKCε$^{-/-}$ mice. RT-PCR for β-actin is shown as loading control. (D) Western blot analysis for PKC family members on brain tissue from PKCε$^{-/-}$ and control mice.

and did not lay down a large amount of adipose tissue with increasing age.

Various aspects of the immune system were investigated in PKCε$^{-/-}$ mice. Thymocytes and T cells developed normally, had an unchanged surface phenotype, and were present at expected numbers. Thymocyte apoptosis to a range of stimuli, including dexamethasone, was comparable to wild type. T cell proliferation to anti-CD3ε antibody or anti-TCRαβ antibody was marginally reduced to ~80% of controls, although the T cell response to antigen after a prior immunization was comparable to wild-type littermates (data not shown). B cells were present at expected numbers with a normal surface phenotype, and serum Ig levels were similar to controls. Basic blood histology and biochemistry revealed no differences between PKCε$^{-/-}$ mice and wild-type littermates (data not shown).

A problem was observed when breeding with homozygous PKCε$^{-/-}$ animals. On average, only one in four female PKCε$^{-/-}$ mice produced a litter, with a second litter from these animals being very rare. On closer examination there was no evidence of a pregnancy of any length in non-litter bearing mothers after a plugging event. On autopsy, ~30% of non-litter bearing female mice presented with distended fluid-filled uteri. Furthermore, even though autoclaved bedding, water, and food were used, a granulocyte/macrophage infiltrate and the presence of copious Gram-negative bacteria such as *E. coli* and various strains of *Proteus* were detected in the uterine fluid. No obvious deformity in uterus structure was observed in healthy PKCε$^{-/-}$ animals (data not shown).

Macrophages from PKCε$^{-/-}$ Mice Generate Reduced NO and Express Lower Levels of NOS-2 mRNA and Protein in Response to In Vitro Challenge with LPS. As PKCε$^{-/-}$ mice were succumbing to *E. coli*–related bacterial infection, it was hypothesized that their response to Gram-negative bacteria was somehow compromised. To test this, macrophages were elicited via intraperitoneal thioglycollate injection and their response to in vitro administration of LPS was assessed measuring nitrite generation as a functional end point. The number of macrophages obtained from PKCε$^{-/-}$ mice were comparable to littermate controls, and the percentage of cells expressing cell-surface levels of both CD14, an integral component of the LPS receptor, and CD11b was similar (Fig. 2 A). At lower doses of LPS, below 200 ng/ml, macrophages from PKCε$^{-/-}$ mice generated significantly lower amounts of NO than macrophages from control animals (Fig. 2 B). However, at substantially higher concentrations of LPS, above 500 ng/ml, a comparable production of NO was detected from both groups. Macrophages can be activated to a greater degree if IFNγ is allowed to act synergistically with LPS. Using a set concentration of both LPS and IFNγ, the generation of NO over a 36-h period was also demonstrated to be significantly reduced in macrophages from PKCε$^{-/-}$ mice when compared with macrophages from wild-type controls (Fig. 2 C). It should be noted that IFNγ treatment alone can result in the generation of NO from macrophages, although this response is lower and delayed with respect to the response observed with LPS (16). In PKCε$^{-/-}$ animals the generation of NO after in vitro IFNγ treatment of elicited macrophages was also reduced in compar-

ison to wild-type littermates (data not shown). The basis of this reduced response to IFNγ in the PKCε$^{-/-}$ mice is presently unclear. However, studies are underway to assess the extent of this defect and to characterize the cellular components involved.

As macrophages are known to generate NO via the up-regulation of the expression of NOS-2, the protein level of NOS-2 was assessed in vitro after the activation of thioglycollate-elicited macrophages by LPS and IFNγ. Fig. 3 A demonstrates that cultured macrophages from PKCε$^{-/-}$ mice displayed a severely reduced level of NOS-2 protein expression after both 18 and 24 h of stimulation when compared with wild-type cells. To verify this decrease in LPS-induced NOS-2 expression, LPS was administered in vivo via an intraperitoneal injection. After 24 h, macrophages were isolated from the peritoneal cavity and again assayed for NOS-2 protein expression. As shown in Fig. 3 B, the extent of induction of NOS-2 protein in response to LPS is severely attenuated in macrophages from PKCε-deficient animals. As NOS-2 activity is mainly controlled at the level of transcription (23), the in vitro expression of NOS-2 RNA in response to LPS plus IFNγ challenge was determined. Fig. 3 C demonstrates that after such a challenge NOS-2 RNA levels were significantly decreased in macrophages from PKCε$^{-/-}$ mice when compared with controls. These data suggest that the reduction in LPS-induced NO generation in macrophages from PKCε$^{-/-}$ mice is a result of the failure to upregulate the expression of both NOS-2 RNA and protein.

Macrophages from PKCε$^{-/-}$ Mice Release Reduced Levels of Proinflammatory Mediators in Response to LPS, and Fail to Undergo Activation-induced Apoptosis. In addition to the synthesis of NO, activated macrophages are known to release a wide range of cytokines and other gene products that promote an inflammatory response and help to initiate adaptive immunity. The production of TNFα, IL-1β, and prostaglandin E_2 (PGE_2) were therefore analyzed after in vitro LPS and IFNγ stimulation of thioglycollate-elicited macrophages. Fig. 4, A–C, clearly demonstrates that mac-

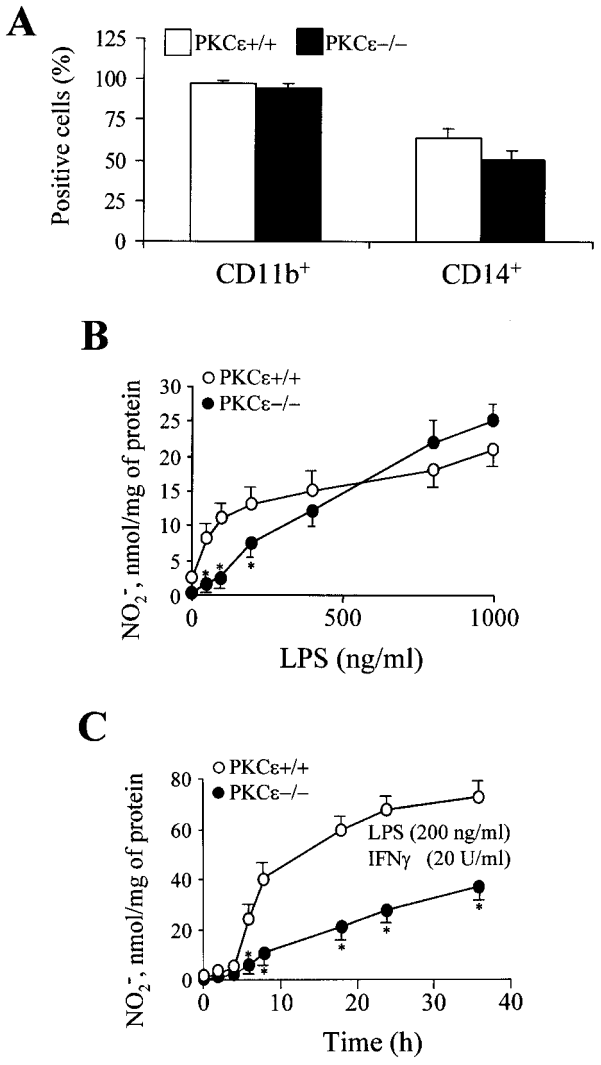

Figure 2. Macrophages from PKCε$^{-/-}$ mice generate less NO in response to LPS challenge. (A) Graphical representation of the percentage of thioglycollate-elicited peritoneal macrophages that expressed cell-surface CD11b and CD14. (B) Graph showing the release of nitrite into the culture medium after the activation of thioglycollate-elicited peritoneal macrophages with increasing concentrations of LPS for 24 h. (C) Graphical view of nitrate release into the culture medium after the activation of thioglycollate-elicited peritoneal macrophages with a fixed concentration of both LPS (200 ng/ml) and IFNγ (20 U/ml) for increasing periods of time. Results show the mean ± SEM of three experiments. The * denotes $P < 0.05$ for experimental vs. wild-type animals for the parameters indicated.

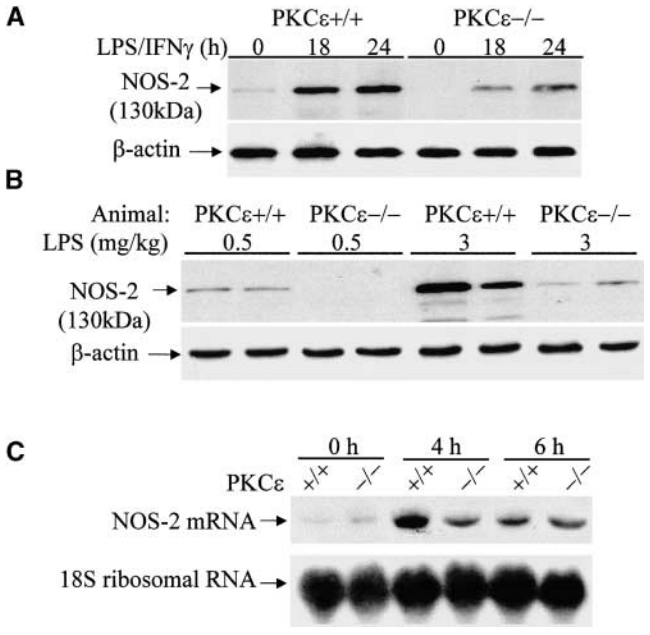

Figure 3. Macrophages from PKCε$^{-/-}$ mice fail to fully induce NOS-2 expression after LPS activation. (A) Western blot for NOS-2 levels in thioglycollate-elicited peritoneal macrophages after 18 or 24 h activation with LPS (200 ng/ml) and IFNγ (20 U/ml). (B) Western blot showing NOS-2 expression in peritoneal macrophages 24 h after an intraperitoneal in vivo challenge with LPS. (C) NOS-2 mRNA levels in macrophages after 4 and 6 h activation with LPS and IFNγ. Loading was normalized by using a probe for 18S ribosomal RNA as a control.

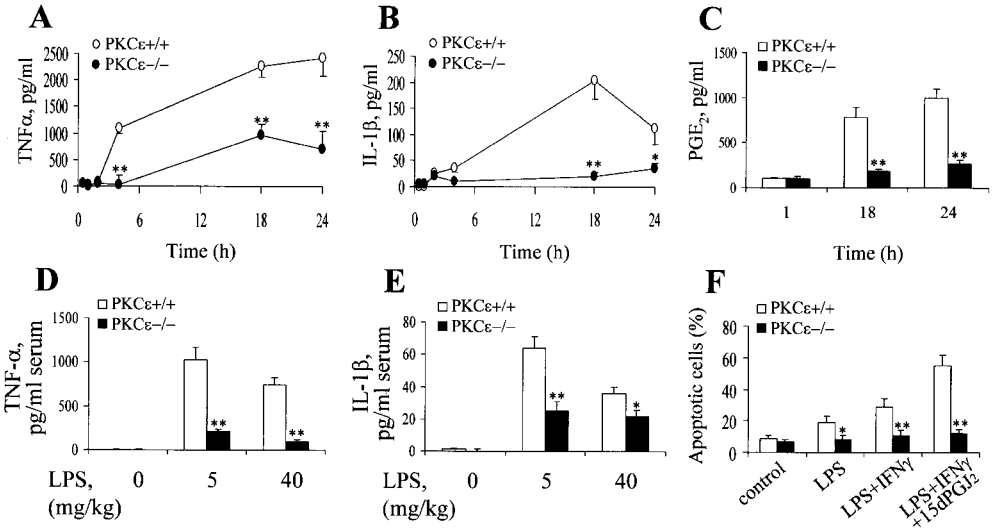

Figure 4. The release of proinflammatory cytokines and prostaglandin E_2 are impaired in PKCε$^{-/-}$ mice. (A–C) Thioglycollate-elicited peritoneal macrophages were activated for the indicated times with 200 ng/ml of LPS and 20 U/ml of IFNγ. The amount of TNF-α, IL-1β, and PGE_2 in the culture medium was then determined. (D–E) Bar graphs demonstrating the serum levels of TNF-α (1 h after injection) and IL-1β (4 h after injection) after the intraperitoneal injection of either 5 mg/kg or 40 mg/kg of LPS. (F) Apoptosis of thioglycollate-elicited peritoneal macrophages 24 h after activation by LPS (200 ng/ml), LPS plus IFNγ (200 ng/ml and 20 U/ml, respectively), or LPS, IFNγ, and 15dPGJ$_2$ (2 μM). Results show the mean ± SEM of three experiments. The * and ** denote $P < 0.05$ and $P < 0.01$, respectively, for experimental vs. wild-type animals, for the parameters indicated.

rophages from PKCε$^{-/-}$ mice generated severely attenuated levels of TNFα, IL-1β, and PGE_2 compared with macrophages from wild-type animals. The release of these proinflammatory mediators was also assessed in vivo after the intraperitoneal administration of LPS after sensitization with D-galactosamine (17). Serum levels of TNFα and IL-1β were both significantly reduced in PKCε$^{-/-}$ mice when compared with the levels observed in littermate controls (Fig. 4, D and E).

Macrophages are known to show characteristic apoptotic cell death at late time points after activation. As an additional indicator of normal macrophage function, the extent of activation-induced apoptosis on thioglycollate-elicited macrophages was analyzed in vitro after 24 h culture in the presence of either LPS, LPS and IFNγ, or LPS, IFNγ, and 15dPGJ$_2$, apoptotic conditions that have been characterized previously (20). As shown in Fig. 4 F, <15% of elicited macrophages from PKCε$^{-/-}$ mice undergo apoptosis in response to any of the three treatments. In contrast, wild-type macrophages show a level of apoptosis of over 20% for each stimulation, with over 50% of the cells undergoing apoptosis in response to the combined action of LPS, IFNγ, and 15dPGJ$_2$. Taken together these results indicate that many mediators of macrophage function in response to LPS are severely disrupted in mice deficient for PKCε.

LPS-activated Macrophages from PKCε$^{-/-}$ Mice Show Significant Impairment of NFκB Activation, and IκB Kinase Activity. Much evidence exists to suggest that the upregulation of NOS-2 requires the transcription factor NFκB (23, 25). Macrophages are known to express NFκB constitutively, but in resting cells NFκB forms an inactive cytoplasmic complex with IκB. On activation, IκB is phosphorylated and degraded, leading to the release of NFκB, which translocates to the nucleus as an active transcription factor. To assess whether the reduction of NOS-2 expression in PKCε$^{-/-}$ mice was due to a decrease in NFκB activation, the presence of active NFκB in macrophage nuclear extracts was analyzed by electrophoretic mobility shift assay (EMSA) after increasing length of LPS stimulation of thioglycollate-elicited cells. The distal κB sequences from the NOS-2 promoter were used to bind the nuclear extracts. In comparison to the clear binding of NFκB (p50.p65) in wild-type lysates, NFκB levels in nuclear extracts from PKCε$^{-/-}$ mice were greatly reduced at all time points analyzed (Fig. 5 A). Supershift assays were performed to verify the nature of the observed bands (data not shown). These results suggest that the failure to activate NFκB in PKCε$^{-/-}$ macrophages could be responsible for the low levels of NOS-2 expression observed in response to LPS stimulation.

The nuclear translocation of NFκB results from the phosphorylation and subsequent degradation of IκB. Macrophages from PKCε$^{-/-}$ mice demonstrate an impaired degradation of IκBα in response to LPS (Fig. 5 B). Consistent with this observation, a reduction in the phosphorylation of IκBα was detected with a specific anti-P(S^{32})IκBα Ab in PKCε-deficient macrophages treated with MG 132 to inhibit proteasome function (21) and hence IκBα degradation (Fig. 5 B). Phosphorylation of IκBα is mediated in part by IκB kinase-2 (IKK-2). Therefore, the activity of IKK-2 in LPS-activated thioglycollate-elicited macrophages was assessed after immunoprecipitation of IKK-2 from cytosolic extracts, using a kinase assay with GST-IκBα and [γ-^{32}P]ATP as substrates. Phosphorylation of the GST-IκBα substrate by IKK-2 was significantly decreased in macrophages from PKCε$^{-/-}$ mice when compared with that of controls (Fig. 5 C). Thus, a failure to activate IKK-2 in LPS-stimulated macrophages could be responsible for the impaired degradation of IκBα and the reduction in active NFκB observed in nuclear extracts from PKCε$^{-/-}$ mice.

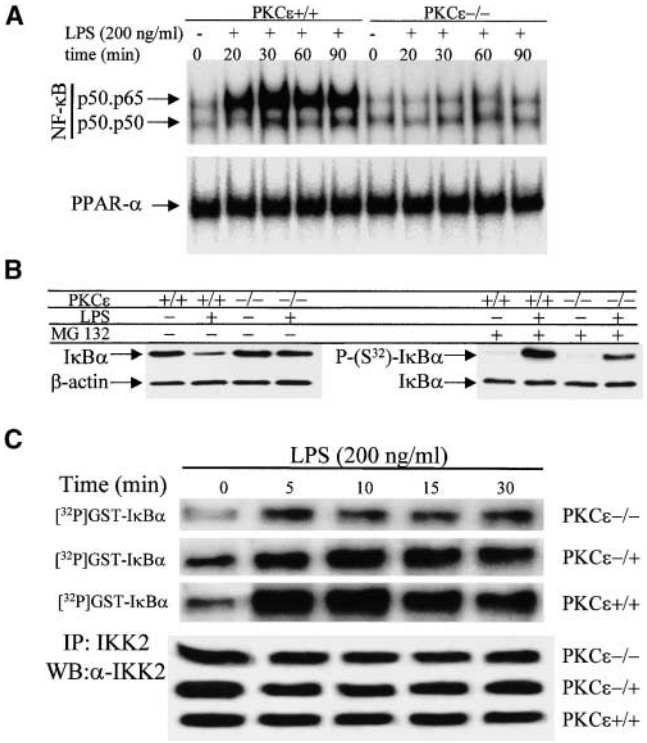

Figure 5. The activation of NF-κB and IKK2 are attenuated in LPS-stimulated macrophages from PKCε$^{-/-}$ mice. (A) Thioglycollate-elicited peritoneal macrophages were activated with 200 ng/ml of LPS, and at the indicated times cytosolic and nuclear protein extracts were prepared. NF-κB activity was determined by EMSA after the binding of nuclear proteins to the distal κB sequence of the murine NOS-2 promoter. The nature of the retained bands was determined by supershift assays (not shown). Normalization was accomplished using the binding of proteins to the PPARα site of acyl CoA oxidase. (B) IκBα levels were determined by Western blot, and the amount of phosphorylated (S^{32})IκBα was evaluated in cells treated with MG 132 (20 μM), and using a specific anti-phospho(S^{32})-IκBα Ab. (C) Macrophages were elicited and treated as above, and at the indicated time points IKK2 was immunoprecipitated from the cytosolic extracts. IKK2 activity was assayed using GST-IκBα (amino acids 1–54) and [γ-^{32}P]ATP as substrates. Results show the incorporation of [^{32}P]phosphate into the substrate, with an aliquot of IKK2 assayed by Western blot to evaluate the level of enzyme.

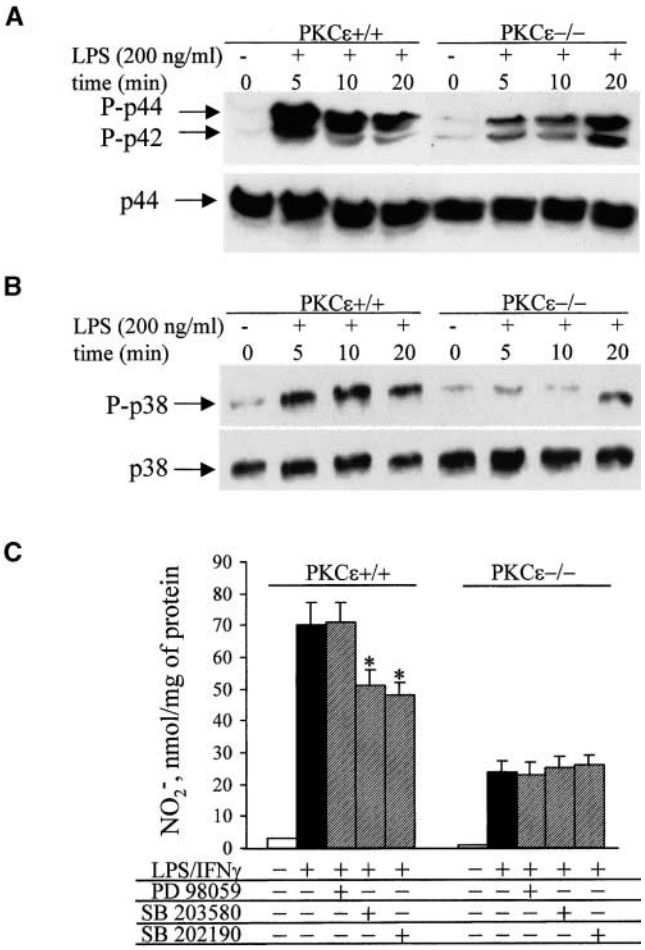

Figure 6. LPS-mediated signaling events are disrupted in macrophages from PKCε$^{-/-}$ mice. (A and B) Thioglycollate-elicited peritoneal macrophages were activated with 200 ng/ml of LPS, and at the indicated times cytosolic and nuclear protein extracts were prepared. The levels of phosphorylated and total p42 ERK and p44 ERK (A), and p38 MAP kinase (B) were determined by Western blot. (C) The effect of p42 and p44 ERK and p38 MAP kinase on the expression of NOS-2 was determined measuring the release of nitrite to the culture medium (24 h) in cells incubated with 50 μM PD 98059, an inhibitor of ERK, and 20 μM of SB203580 and SB20190, inhibitors of p38 MAP kinase. Results show the mean ± SEM of three experiments. The * denotes $P < 0.05$ with respect to the LPS (200 ng/ml) and IFNγ (20 U/ml) responses in control vs. experimental animals.

LPS-activated Macrophages from PKCε$^{-/-}$ Mice Display Defects in a Number of Cellular Signaling Pathways. Previous work has implicated several signaling pathways in the up-regulation of expression of genes such as NOS-2, TNFα, and IL-1β after the LPS stimulation of macrophages. Two such pathways are those involving the ERK1/2 MAP kinases and the family of p38 MAP kinases. The activation of these kinases was therefore assessed by detection of the phosphorylated forms of p44ERK, p42ERK, and p38 in LPS-stimulated macrophage cytosolic extracts. The amount of phosphorylated p44, p42, and p38 is clearly reduced in extracts from LPS-stimulated macrophages from PKCε$^{-/-}$ mice, particularly at early time points after stimulation (Fig. 6, A and B). The relevance of this reduction in LPS-induced p44/p42ERK and p38 activation with respect to NO synthesis was evaluated. Whereas PD 98059, an inhibitor of ERK, was unable to modify NO synthesis in response to LPS in macrophages from wild-type animals, SB 203580 and SB 202190, two inhibitors of p38 MAPK, significantly inhibited NO synthesis in activated macrophages from PKCε$^{+/+}$ mice (Fig. 6 C), confirming previous data (26). However, neither SB 203580 nor SB 202190 affected the already lowered synthesis of NO in PKCε$^{-/-}$ mice (Fig. 6 C). These results suggest that although both the ERK and p38 MAP kinase signaling cascades are attenuated in PKCε$^{-/-}$ mice in response to LPS, only the p38 MAP kinase pathway is directly involved in NO production in a PKCε-dependent manner.

PKCε$^{-/-}$ Mice Are Less Resistant to Gram-negative and Gram-positive Bacterial Challenge. As female PKCε$^{-/-}$ mice displayed an unexpected incidence of uterine Gram-

negative bacterial infection, and macrophages from PKCε$^{-/-}$ mice were demonstrated to have a severely attenuated response to LPS stimulation, it was hypothesized that PKCε-deficient animals would be more sensitive to Gram-negative bacteria than wild-type controls. To assess this possibility directly, a controlled *E. coli* bacterial infection was administered intravenously to both PKCε$^{-/-}$ and wild-type mice. At a bacterial dose of 3×10^5 pathogens per gram, ~40% of the control animals survived for at least 20 d after infection. In contrast, all PKCε$^{-/-}$ mice had died by day 8 (median; 4.6 and 25.3 d for PKCε$^{-/-}$ and wild-type, respectively; Fig. 7 A). At the higher bacterial dose of 3×10^6 pathogens per gram, all animals from the wild-type group had died by day 3. However again, the PKCε$^{-/-}$ mice showed a decreased resistance to infection, as no animal survived beyond the first day (Fig. 7 B). Interestingly, when animals were injected with 3×10^5 Gram-positive *S. aureus* per gram of body weight, a difference in survival was also observed between PKCε$^{-/-}$ and wild-type animals (median; 6.8 and 21 d, respectively; Fig. 7 C). These results clearly demonstrate that mice deficient for PKCε are more sensitive to both Gram-negative and Gram-positive bacterial infection than wild-type controls, and that this increased sensitivity to infection can significantly decrease the likelihood of bacterial clearance and survival.

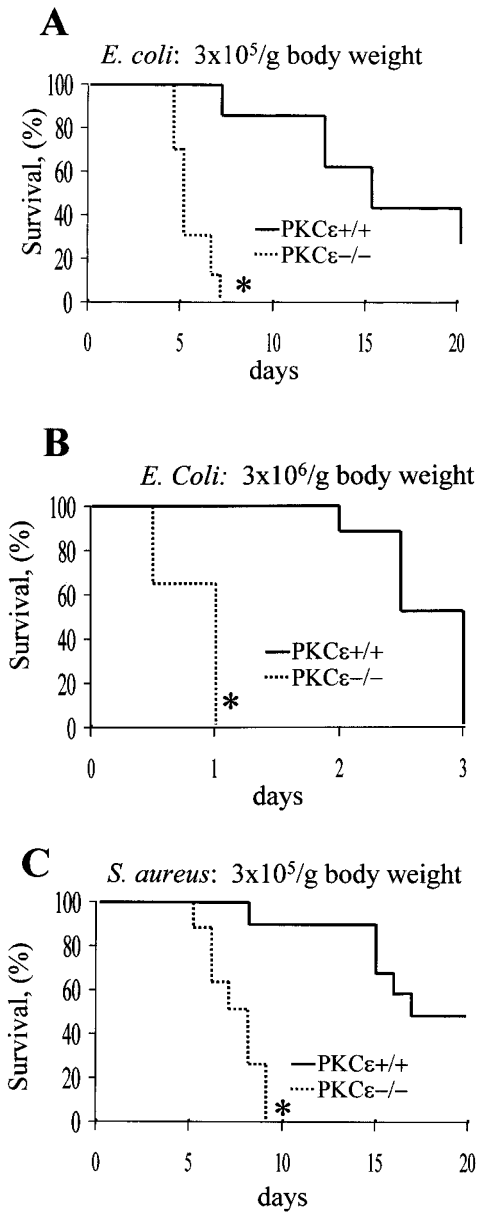

Figure 7. PKCε$^{-/-}$ mice are more sensitive to Gram-negative and Gram-positive bacterial challenge. Animals (n = 7–11 for each group) were injected intravenously with either (A) 3×10^5 or (B) 3×10^6 *E. coli* per gram of body weight, or (C) 3×10^5 *S. aureus* per gram of body weight. Survival of the mice was monitored for up to 20 d. Data were analyzed using the Kaplan-Meier plot. The * denotes $P < 0.05$ for experimental vs. wild-type survival times.

Discussion

The studies presented here indicate that PKCε plays a major role in macrophage biology. Although the absence of PKCε did not seem to influence the differentiation of monocytes and macrophages from bone marrow precursors, or affect extravasation of macrophages in response to proinflammatory stimuli, a major defect in the ability of extravased macrophages to respond to LPS was observed. At low concentrations of LPS (ca. 200 ng/ml) the generation of NO from PKCε$^{-/-}$ macrophages was severely reduced. The generation of NO, TNFα, and IL-1β was also decreased after the synergistic activation of PKCε$^{-/-}$ macrophages with LPS and IFNγ (23, 27). Furthermore, several LPS-activated signaling pathways, involving IKK-2, IκBα, NFκB, the ERK MAP kinases, and p38 MAP kinase were attenuated in PKCε-deficient cells. Taken together, these results suggest that PKCε has a critical function in the regulation of a number of signaling pathways that mediate various aspects of macrophage activation.

Macrophages constitute a key component of the innate immune system, having the ability to recognize relatively invariant pathogen-associated molecular patterns from a range of bacteria and fungi (28–31). As a defensive response to these microbial structures, macrophages can release a diverse array of bioactive molecules at sites of infection. These effector molecules include reactive oxygen and nitrogen species, prostaglandins, and matrix metalloproteinases (32–36). Macrophages can also contribute to the initiation of the adaptive immune response by presenting antigen to T cells and by expressing costimulatory molecules, such as B7, and a range of cytokines, such as IL-1β, IL-6, IL-10, and TNFα, that instruct the adaptive immune system about the general nature of the invading pathogen (28, 35).

LPS is a component of the outer membrane of Gram-negative bacteria that is recognized as a pathogen-associated molecular pattern by macrophages (35). The major LPS receptor complex has been demonstrated to consist of a serum protein known as LPS-binding protein, a GPI-linked surface protein known as CD14, and the toll-like receptor-4 (TLR-4) transmembrane protein in association with the product of the MD-2 gene (28, 37–40). The percentage of

macrophages expressing CD14 (and mouse embryonic fibroblasts, data not shown) from PKCε$^{-/-}$ mice is comparable to that observed in wild-type controls. Furthermore, the apparent affinity for LPS and anti-CD14 mAbs was also unaltered on macrophages from PKCε-deficient animals (data not shown). This would imply that PKCε has a role downstream of the CD14/TLR-4 complex. However, the defect in LPS-induced macrophage activation in PKCε$^{-/-}$ mice is not as severe as that observed in TLR-4$^{-/-}$ animals, as some NO generation is observed at low concentrations of LPS and NO production is comparable to wild-type levels at much higher concentrations of LPS. This would suggest that PKCε is not absolutely essential for LPS-mediated signaling, but instead could have a modulatory role, amplifying the signaling cascade when levels of LPS are limiting.

The full complement of downstream signaling events that are initiated by LPS receptor binding are still not fully understood. However, evidence exists to suggest the involvement of Src-kinases (41), G proteins (42), phospholipase C (43–45), and protein kinase A (46). Several studies have also implicated MAP kinase activation as a critical event in LPS-mediated signaling (47–51). We have demonstrated that the extent of both p38 MAP kinase activation and ERK-1/ERK-2 MAP kinase activation is significantly decreased after LPS-stimulation of PKCε$^{-/-}$ macrophages. Furthermore, our results suggest that the PKCε-dependent activation of the p38 MAP kinase pathway partially induces NO production (26). This would suggest that the role of PKCε is upstream of phosphorylation events that activate these kinases, and implicates PKCε in the activation of a number of diverse signaling cascades. In this regard, the PKCε-mediated activation of the MAP kinase pathway, leading to the nuclear translocation of NFκB, has recently been demonstrated in adult rabbit cardiomyocytes (52).

The synthesis of NO has been extensively studied in macrophages. It is known that NO generation is dependent on the cellular levels of NOS-2, and that the upregulation of NOS-2 expression is in turn dependent on NFκB binding at κB sites located in the NOS-2 promoter (25, 53). In resting cells, NFκB forms an inactive complex with the inhibitor IκB in the cytosol. On activation, the phosphorylation and degradation of IκB by an IκB kinase (IKK) results in the nuclear translocation of NFκB and the activation of target genes (54–57). In RAW 264.7 cells, PKCε expression was demonstrated to be sufficient for NFκB activation and NOS-2 induction (16). Consistent with these observations, our data demonstrate that LPS-induced NFκB translocation and induction of NOS-2 expression are both severely disrupted in macrophages from PKCε$^{-/-}$ mice. Furthermore, IκBα phosphorylation and degradation is reduced, and IKK-2 activity is significantly decreased in the absence of PKCε.

At present, the signaling events upstream of IKK are not fully understood, although the involvement of several kinases has been implicated, including NFκB-activating kinase (NAK) (58) and TGFβ-activated kinase (TAK-1) possibly via the activation of NFκB-inducing kinase (NIK) (59). Interestingly, the expression of a catalytically inactive NAK protein was shown to specifically inhibit activation of NFκB by PKCε, but not by PKCα or PKCθ (58). In addition, this NAK mutant blocked NFκB activation by PDGF, which has been reported to signal through PKCε (60). However, the authors also reported that although a dominant negative IKK-2 mutant blocked activation of NFκB by LPS, the catalytically inactive NAK had little effect. This would suggest that the activation of IKK-2 is probably mediated by a number of signaling pathways that may not all be influenced by PKCε.

TAK-1 has recently been implicated in a complex signaling cascade from the LPS receptor TLR-4 which involves MyD88, IRAK, TRAF-6, ECSIT, and TAB2 (61–66). It is presently unclear exactly how PKCε could interact with this pathway. However, it is worth noting that the TLR-2 receptor-induced signaling cascade has been shown to share many of these intermediary molecules (67). As the TLR-2 complex is known to mediate potent macrophage responses to pathogens such as Gram-positive bacteria and mycoplasma (68–70), and as PKCε$^{-/-}$ mice displayed an increased sensitivity to Gram-positive bacterial challenge, it is tempting to speculate that PKCε could function at a point common to both the TLR-4 and TLR-2 cascades. Further work is underway to establish the basis of the increased sensitivity to Gram-positive bacteria observed in this study.

The synthesis of LPS-induced proinflammatory mediators such as NO, TNFα, and IL-1β are required for the full activation of macrophage function and the correct initiation of an appropriate immune response to a Gram-negative bacterial infection (28, 35, 71–73). Our results clearly demonstrate that in mice lacking PKCε the generation of LPS-induced proinflammatory mediators is notably diminished. This would predict that PKCε$^{-/-}$ mice would be sensitive to infection by Gram-negative bacteria such as *E. coli*. Consistent with this hypothesis, we observed a frequent incidence of *E. coli* infection in the uteri of PKCε$^{-/-}$ animals, a type of infection that was never observed in control animals over a similar period. Furthermore, in a controlled intravenous infection of animals with *E. coli*, survival times were markedly reduced in the absence of PKCε. However, we also observed a decreased macrophage response to IFNγ challenge, and an increased sensitivity to Gram-positive bacteria in PKCε-deficient animals. Taken together, these data conclude that PKCε is a critical mediator of several signaling cascades in activated macrophages, and that in the absence of PKCε, the successful initiation of an effective immune response against a range of bacterial pathogen is severely compromised.

The authors thank Dr. Rosalía Díez and Gloria Molero from the Faculty of Pharmacy, Madrid for help to perform the in vivo experiments. We also thank Ian Rosewell for blastocyst injections, Gill Hutchinson and Julie Bee for thioglycollate and LPS injections, and Caetano Reis e Sousa, Nancy Hogg, and Doreen Cantrell for critical evaluation of the manuscript.

This work was supported by the Imperial Cancer Research

Fund, and grants FEDER 2FD-1997-1432 from Comisión Interministerial de Ciencia y Tecnología (CICYT) and PM98-0120 from Dirección General de Enseñanza Superior e Investigación Científica, Spain. F. Otto was supported by Deutsche Forschungsgemeinschaft grant Ot 134/1-1.

Submitted: 26 February 2001
Revised: 4 September 2001
Accepted: 21 September 2001

References

1. Mellor, H., and P.J. Parker. 1998. The extended protein kinase C superfamily. *Biochem. J.* 332:281–292.
2. Parekh, D.B., W. Ziegler, and P.J. Parker. 2000. Multiple pathways control protein kinase C phosphorylation. *EMBO J.* 19:496–503.
3. Abeliovich, A., C. Chen, Y. Goda, A.J. Silva, C.F. Stevens, and S. Tonegawa. 1993. Modified hippocampal long-term potentiation in PKC-γ mutant mice. *Cell.* 75:1253–1262.
4. Leitges, M., C. Schmedt, R. Guinamard, J. Davoust, S. Schaal, S. Stabel, and A. Tarakhovsky. 1996. Immunodeficiency in protein kinase C β-deficient mice. *Science.* 273: 788–791.
5. Khasar, S.G., Y.H. Lin, A. Martin, J. Dadgar, T. McMahon, D. Wang, B. Hundle, K.O. Aley, W. Isenberg, G. McCarter, et al. 1999. A novel nociceptor signaling pathway revealed in protein kinase C ε mutant mice. *Neuron.* 24:253–260.
6. Sun, Z., C.W. Arendt, W. Ellmeier, E.M. Schaeffer, M.J. Sunshine, L. Gandhi, J. Annes, D. Petrzilka, A. Kupfer, P.L. Schwartzberg, and D.R. Littman. 2000. PKC-θ is required for TCR-induced NF-κB activation in mature but not immature T lymphocytes. *Nature.* 404:402–407.
7. Iwata, M., R. Iseki, K. Sato, Y. Tozawa, and Y. Ohoka. 1994. Involvement of protein kinase C-ε in glucocorticoid-induced apoptosis in thymocytes. *Int. Immunol.* 3:431–438.
8. Gómez, J., C. Pitton, A. García, A. Martinez de Aragón, A. Silva, and A. Rebollo. 1995. The zeta isoform of protein kinase C controls interleukin-2-mediated proliferation in a murine T cell line: evidence for an additional role of protein kinase C ε and β. *Exp. Cell Res.* 218:105–113.
9. Sands, W.A., V. Bulut, A. Severn, D. Xu, and F.Y. Liew. 1994. Inhibition of nitric oxide synthesis by interleukin-4 may involve inhibiting the activation of protein kinase C ε. *Eur. J. Immunol.* 24:2345–2350.
10. Diaz-Guerra, M.J., O.G. Bodelon, M. Velasco, R. Whelan, P.J. Parker, and L. Bosca. 1996. Up-regulation of protein kinase C-ε promotes the expression of cytokine-inducible nitric oxide synthase in RAW 264.7 cells. *J. Biol. Chem.* 271: 32028–32033.
11. Lin, M.Q., and Z.L. Chang. 1996. LPS and PMA induced PKC-α and PKC-ε activation and translocation in murine peritoneal macrophages. *Shih Yen Sheng Wu Hsueh Pao.* 4:429–434.
12. Shapira, L., V.L. Sylvia, A. Halabi, W.A. Soskolne, T.E. Van Dyke, D.D. Dean, B.D. Boyan, and Z. Schwartz. 1997. Bacterial lipopolysaccharide induces early and late activation of protein kinase C in inflammatory macrophages by selective activation of PKC-ε. *Biochem. Biophys. Res. Commun.* 240: 629–634.
13. Baxter, G.T., D.L. Miller, R.C. Kuo, H.G. Wada, and J.C. Owicki. 1992. PKC ε is involved in granulocyte-macrophage colony-stimulating factor signal transduction: evidence from microphysiometry and antisense oligonucleotide experiments. *Biochemistry.* 31:10950–10954.
14. Valledor, A.F., J. Xaus, M. Comalada, C. Soler, and A. Celada. 2000. Protein kinase C ε is required for the induction of mitogen-activated protein kinase phosphatase-1 in lipopolysaccharide-stimulated macrophages. *J. Immunol.* 164: 29–37.
15. Larsen, E.C., J.A. DiGennaro, N. Saito, S. Mehta, D.J. Loegering, J.E. Mazurkiewicz, and M.R. Lennartz. 2000. Differential requirement for classic and novel PKC isoforms in respiratory burst and phagocytosis in RAW 264.7 cells. *J. Immunol.* 165:2809–2817.
16. Diaz-Guerra, M.J.M., A. Castrillo, P. Martin-Sanz, and L. Bosca. 1999. Negative regulation by protein tyrosine phosphatase of IFN-γ-dependent expression of inducible nitric oxide synthase. *J. Immunol.* 162:6776–6783.
17. Galanos, C., M.A. Freudenberg, and W. Reutter. 1979. Galactosamine-induced sensitization to the lethal effects of endotoxin. *Proc. Natl. Acad. Sci. USA.* 76:5939–5943.
18. Miethke, T., C. Wahl, K. Heeg, B. Echtenacher, P.H. Krammer, and H. Wagner. 1992. T cell-mediated lethal shock triggered in mice by the superantigen staphylococcal enterotoxin B: critical role of tumor necrosis factor. *J. Exp. Med.* 175:91–98.
19. Hortelano, S., A.M. Alvarez, and L. Bosca. 1999. Nitric oxide induces tyrosine nitration and release of cytochrome c preceding an increase of mitochondrial transmembrane potential in macrophages. *FASEB J.* 13:2311–2317.
20. Hortelano, S., A. Castrillo, A.M. Alvarez, and L. Bosca. 2000. Contribution of cyclopentenone prostaglandins to the resolution of inflammation through the potentiation of apoptosis in activated macrophages. *J. Immunol.* 165:6525–6531.
21. Castrillo, A., M.J. Diaz-Guerra, S. Hortelano, P. Martin-Sanz, and L. Bosca. 2000. Inhibition of IκB kinase and IκB phosphorylation by 15-deoxy-delta^{12,14}-prostaglandin J_2 in activated murine macrophages. *Mol. Cell Biol.* 20:1692–1698.
22. Velasco, M., M.J. Diaz-Guerra, P. Martin-Sanz, A. Alvarez, and L. Bosca. 1997. Rapid Up-regulation of IκB-β and abrogation of NF-κB activity in peritoneal macrophages stimulated with lipopolysaccharide. *J. Biol. Chem.* 272:23025–23030.
23. Xie, Q.W., R. Whisnant, and C. Nathan. 1993. Promoter of the mouse gene encoding calcium-independent nitric oxide synthase confers inducibility by interferon-γ and bacterial lipopolysaccharide. *J. Exp. Med.* 177:1779–1784.
24. Dowell, P., V.J. Peterson, T.M. Zabriskie, and M. Leid. 1997. Ligand-induced peroxisome proliferator-activated receptor α conformational change. *J. Biol. Chem.* 272:2013–2020.
25. Xie, Q.W., Y. Kashiwabara, and C. Nathan. 1994. Role of transcription factor NF-κB/Rel in induction of nitric oxide synthase. *J. Biol. Chem.* 269:4705–4708.
26. Chen, C.C., and J.K. Wang. 1999. p38 but not p44/42 mitogen-activated protein kinase is required for nitric oxide synthase induction mediated by lipopolysaccharide. *Mol. Pharmacol.* 55:481–488.
27. Lowenstein, C.J., E.W. Alley, P. Raval, A.M. Snowman, S.H. Snyder, S.W. Russell, and W.J. Murphy. 1993. Macrophage nitric oxide synthase gene: two upstream regions mediate induction by interferon-γ and lipopolysaccharide. *Proc. Natl. Acad. Sci. USA.* 90:9730–9734.
28. Ulevitch, R.J., and P.S. Tobias. 1995. Receptor-dependent mechanisms of cell stimulation by bacterial endotoxin. *Annu.*

Rev. Immunol. 13:437–457.
29. Sweet, M.J., and D.A. Hume. 1996. Endotoxin signal transduction in macrophages. *J. Leukoc. Biol.* 60:8–26.
30. Vadiveloo, P.K. 1999. Macrophages, proliferation, activation, and cell cycle proteins. *J. Leukoc. Biol.* 66:579–582.
31. Kitchens, R.L. 2000. Role of CD14 in cellular recognition of bacterial lipopolysaccharides. *Chem. Immunol.* 74:61–82.
32. Nathan, C. 1992. Nitric oxide as a secretory product of mammalian cells. *FASEB J.* 6:3051–3064.
33. Nathan, C. 1995. Natural resistance and nitric oxide. *Cell.* 82:873–876.
34. MacMicking, J., Q.W. Xie, and C. Nathan. 1997. Nitric oxide and macrophage function. *Annu. Rev. Immunol.* 15:323–350.
35. Downey, J.S., and J. Han. 1998. Cellular activation mechanisms in septic shock. *Front. Biosci.* 3:468–476.
36. Hoffmann, J.A., F.C. Kafatos, C.A. Janeway, and R.A. Ezekowitz. 1999. Phylogenetic perspectives in innate immunity. *Science.* 284:1313–1318.
37. Poltorak, A., X. He, I. Smirnova, M.Y. Liu, C.V. Huffel, X. Du, D. Birdwell, E. Alejos, M. Silva, C. Galanos, et al. 1998. Defective LPS signaling in C3H/HeJ and C57BL/10ScCr mice: mutations in Tlr4 gene. *Science.* 282:2085–2088.
38. Hoshino, K., O. Takeuchi, T. Kawai, H. Sanjo, T. Ogawa, Y. Takeda, K. Takeda, and S. Akira. 1999. Cutting edge: Toll-like receptor 4 (TLR4)-deficient mice are hyporesponsive to lipopolysaccharide: evidence for TLR4 as the Lps gene product. *J. Immunol.* 162:3749–3752.
39. Chow, J.C., D.W. Young, D.T. Golenbock, W.J. Christ, and F. Gusovsky. 1999. Toll-like receptor-4 mediates lipopolysaccharide-induced signal transduction. *J. Biol. Chem.* 274:10689–10692.
40. Shimazu, R., S. Akashi, H. Ogata, Y. Nagai, K. Fukudome, K. Miyake, and M. Kimoto. 1999. MD-2, a molecule that confers lipopolysaccharide responsiveness on Toll-like receptor 4. *J. Exp. Med.* 189:1777–1782.
41. Boulet, I., S. Ralph, E. Stanley, P. Lock, A.R. Dunn, S.P. Green, and W.A. Phillips. 1992. Lipopolysaccharide- and interferon-gamma-induced expression of hck and lyn tyrosine kinases in murine bone marrow-derived macrophages. *Oncogene.* 4:703–710.
42. Daniel-Issakani, S., A.M. Spiegel, and B. Strulovici. 1989. Lipopolysaccharide response is linked to the GTP binding protein, Gi2, in the promonocytic cell line U937. *J. Biol. Chem.* 264:20240–20247.
43. Chen, B.D., T.H. Chou, and L. Sensenbrenner. 1993. Downregulation of M-CSF receptors by lipopolysaccharide in murine peritoneal exudate macrophages is mediated through a phospholipase C dependent pathway. *Exp. Hematol.* 5:623–628.
44. Yamamoto, H., K. Hanada, and M. Nishijima. 1997. Involvement of diacylglycerol production in activation of nuclear factor κB by a CD14-mediated lipopolysaccharide stimulus. *Biochem. J.* 325:223–228.
45. Monick, M.M., A.B. Carter, G. Gudmundsson, R. Mallampalli, L.S. Powers, and G.W. Hunninghake. 1999. A phosphatidylcholine-specific phospholipase C regulates activation of p42/44 mitogen-activated protein kinases in lipopolysaccharide-stimulated human alveolar macrophages. *J. Immunol.* 162:3005–3012.
46. Shapira, L., S. Takashiba, C. Champagne, S. Amar, and T.E. Van Dyke. 1994. Involvement of protein kinase C and protein tyrosine kinase in lipopolysaccharide-induced TNF-α and IL-1β production by human monocytes. *J. Immunol.* 153:1818–1824.
47. Weinstein, S.L., J.S. Sanghera, K. Lemke, A.L. DeFranco, and S.L. Pelech. 1992. Bacterial lipopolysaccharide induces tyrosine phosphorylation and activation of mitogen-activated protein kinases in macrophages. *J. Biol. Chem.* 267:14955–14962.
48. Reimann, T., D. Büscher, R.A. Hipskind, S. Krautwald, M.L. Lohmann-Matthes, and M. Baccarini. 1994. Lipopolysaccharide induces activation of the Raf-1/MAP kinase pathway. A putative role for Raf-1 in the induction of the IL-1β and the TNF-α genes. *J. Immunol.* 153:5740–5749.
49. Geppert, T.D., C.E. Whitehurst, P. Thompson, and B. Beutler. 1994. Lipopolysaccharide signals activation of tumor necrosis factor biosynthesis through the ras/raf-1/MEK/MAPK pathway. *Mol. Med.* 1:93–103.
50. Han, J., J.D. Lee, J. Bibbs, and R.J. Ulevitch. 1994. A MAP kinase targeted by endotoxin and hyperosmolarity in mammalian cells. *Science.* 265:808–811.
51. Hambleton, J., S.L. Weinstein, L. Lem, and A.L. DeFranco. 1996. Activation of c-Jun N-terminal kinase in bacterial lipopolysaccharide-stimulated macrophages. *Proc. Natl. Acad. Sci. USA.* 93:2774–2778.
52. Li, R.C., P. Ping, J. Zhang, W.B. Wead, X. Cao, J. Gao, Y. Zheng, S. Huang, J. Han, and R. Bolli. 2000. PKC-ϵ modulates NF-κB and AP-1 via mitogen-activated protein kinases in adult rabbit cardiomyocytes. *Am. J. Physiol. Heart Circ. Physiol.* 279:H1679–H1689.
53. Tak, P.P., and G.S. Firestein. 2001. NF-κB: a key role in inflammatory diseases. *J. Clin. Invest.* 107:7–11.
54. Mercurio, F., H. Zhu, B.W. Murray, A. Shevchenko, B.L. Bennett, J. Li, D.B. Young, M. Barbosa, M. Mann, A. Manning, and A. Rao. 1997. IKK-1 and IKK-2: cytokine-activated IκB kinases essential for NF-κB activation. *Science.* 278:860–866.
55. May, M.J., and S. Ghosh. 1998. Signal transduction through NF-κB. *Immunol. Today.* 19:80–88.
56. Zandi, E., Y. Chen, and M. Karin. 1998. Direct phosphorylation of IκB by IKK-α and IKK-β: discrimination between free and NF-κB-bound substrate. *Science.* 281:1360–1363.
57. Karin, M. 1999. The beginning of the end: IκB kinase (IKK) and NF-κB activation. *J. Biol. Chem.* 274:27339–27342.
58. Tojima, Y., A. Fujimoto, M. Delhase, Y. Chen, S. Hatakeyama, K. Nakayama, Y. Kaneko, Y. Nimura, N. Motoyama, K. Ikeda, et al. 2000. NAK is an IκB kinase-activating kinase. *Nature.* 404:778–782.
59. Ninomiya-Tsuji, J., K. Kishimoto, A. Hiyama, J. Inoue, Z. Cao, and K. Matsumoto. 1999. The kinase TAK-1 can activate the NIK-1 κB as well as the MAP kinase cascade in the IL-1 signalling pathway. *Nature.* 398:252–256.
60. Moriya, S., A. Kazlauskas, K. Akimoto, S. Hirai, K. Mizuno, T. Takenawa, Y. Fukui, Y. Watanabe, S. Ozaki, and S. Ohno. 1996. Platelet-derived growth factor activates protein kinase C through redundant and independent signaling pathways involving phospholipase C or phosphatidylinositol 3-kinase. *Proc. Natl. Acad. Sci. USA.* 93:151–155.
61. Medzhitov, R., P. Preston-Hurlburt, E. Kopp, A. Stadlen, C. Chen, S. Ghosh, and C.A. Janeway. 1998. MyD88 is an adaptor protein in the hToll/IL-1 receptor family signaling pathways. *Mol. Cell.* 2:253–258.
62. Lomaga, M.A., W.C. Yeh, I. Sarosi, G.S. Duncan, C. Furlonger, A. Ho, S. Morony, C. Capparelli, G. Van, S. Kauf-

man, A. van der Heiden, et al. 1999. TRAF6 deficiency results in osteopetrosis and defective interleukin-1, CD40, and LPS signalling. *Genes Dev.* 13:1015–1024.
63. Kopp, E., R. Medzhitov, J. Carothers, C. Xiao, I. Douglas, C.A. Janeway, and S. Ghosh. 1999. ECSIT is an evolutionarily conserved intermediate in the Toll/IL-1 signal transduction pathway. *Genes Dev.* 13:2059–2071.
64. Thomas, J.A., J.L. Allen, M. Tsen, T. Dubnicoff, J. Danao, X.C. Liao, Z. Cao, and S.A. Wasserman. 1999. Impaired cytokine signaling in mice lacking the IL-1 receptor-associated kinase. *J. Immunol.* 163:978–984.
65. Takaesu, G., S. Kishida, A. Hiyama, K. Yamaguchi, H. Shibuya, K. Irie, J. Ninomiya-Tsuji, and K. Matsumoto. 2000. TAB2, a novel adapter protein, mediates activation of TAK1 MAPKKK by linking TAK1 to TRAF6 in the IL-1 signal transduction pathway. *Mol. Cell.* 5:649–658.
66. Irie, T., T. Muta, and K. Takeshige. 2000. TAK1 mediates an activation signal from toll-like receptor(s) to nuclear factor-κB in lipopolysaccharide-stimulated macrophages. *FEBS Lett.* 467:160–164.
67. Takeuchi, O., A. Kaufmann, K. Grote, T. Kawai, K. Hoshino, M. Morr, P.F. Muhlradt, and S. Akira. 2000. Cutting edge: preferentially the R-stereoisomer of the mycoplasmal lipopeptide macrophage-activating lipopeptide-2 activates immune cells through a toll-like receptor 2- and MyD88-dependent signalling pathway. *J. Immunol.* 164:554–557.
68. Yoshimura, A., E. Lien, R.R. Ingalls, E. Tuomanen, R. Dziarski, and D. Golenbock. 1999. Cutting edge: recognition of Gram-positive bacterial cell wall components by the innate immune system occurs via Toll-like receptor 2. *J. Immunol.* 163:1–5.
69. Lien, E., T.J. Sellati, A. Yoshimura, T.H. Flo, G. Rawadi, R.W. Finberg, J.D. Carroll, T. Espevik, R.R. Ingalls, J.D. Radolf, and D.T. Golenbock. 1999. Toll-like receptor 2 functions as a pattern recognition receptor for diverse bacterial products. *J. Biol. Chem.* 274:33419–33425.
70. Takeuchi, O., K. Hoshino, T. Kawai, H. Sanjo, H. Takada, T. Ogawa, K. Takeda, and S. Akira. 1999. Differential roles of TLR2 and TLR4 in recognition of gram-negative and gram-positive bacterial cell wall components. *Immunity.* 11: 443–451.
71. Malinin, N.L., M.P. Boldin, A.V. Kovalenko, and D. Wallach. 1997. MAP3K-related kinase involved in NF-κB induction by TNF, CD95 and IL-1. *Nature.* 385:540–544.
72. van der Bruggen, T., S. Nijenhuis, E. van Raaij, J. Verhoef, and B.S. van Asbeck. 1999. Lipopolysaccharide-induced tumor necrosis factor alpha production by human monocytes involves the raf-1/MEK1-MEK2/ERK1-ERK2 pathway. *Infect. Immun.* 67:3824–3829.
73. Baud, V., Z.G. Liu, B. Bennett, N. Suzuki, Y. Xia, and M. Karin. 1999. Signalling by pro-inflammatory cytokines: oligomerisation of TRAF2 and TRAF6 is sufficient for JNK and IKK activation and target gene induction via an amino-terminal effector domain. *Genes Dev.* 13:1297–1308.